

# Angular Broadening of Nearby Pulsars

M. C. Britton, C. R. Gwinn, and M. J. Ojeda

Physics Department, University of California, Santa Barbara, California 93106, USA.

## ABSTRACT

We conducted a very long baseline interferometric (VLBI) observation of 5 nearby pulsars and did not resolve the scattering disks of any of these sources. Using our upper limits on the angular diameters of these scattering disks and published values of the broadening times and proper motion velocities, we constrain the possible distributions of scattering material. The material responsible for scattering these sources is neither uniformly distributed nor concentrated at the surface of the Local Bubble. We argue that these pulsars themselves influence their environments to produce this scattering material.

*Subject headings:* turbulence, scattering - ISM: structure - pulsars: general - techniques: interferometric

## 1. INTRODUCTION

Fluctuations in the interstellar electron density scatter radio waves and cause angular broadening of radio sources. The angular sizes of these broadened sources contain information about the material responsible for scattering. Rao & Ananthakrishnan (1984) found that the angular diameters of low-latitude ( $|b| < 10^\circ$ ) radio sources tend to be larger in the direction of the galactic center. Dennison et al (1984) found large variations in the angular diameters of low-latitude extragalactic radio sources along nearby lines of sight. Some low-latitude sources are scattered by HII regions (Moran et al. 1990, Molnar et al. 1995) or supernova remnants (Spangler et al. 1986). These results suggest that the scattering material in the disk of our galaxy contains both an extended component and localized features.

Pulsars are weak radio sources, but permit observation of the temporal broadening of their pulses as well as angular broadening. Cordes, Weisberg, & Boriakoff (1985) found strong variations in the temporal broadening of pulsars along nearby lines of sight. Gwinn, Bartel, & Cordes (1993) have compared the angular broadening and temporal broadening of pulsars to distinguish between different distributions of scattering material. They conclude

that the scattering properties of several distant pulsars are consistent with a uniform distribution of scattering material. The Vela pulsar is a notable exception; this young pulsar is scattered by its supernova remnant (Desai et al. 1992).

Because of the small scale height of the galactic disk, radio sources at high galactic latitudes ( $|b| > 10^\circ$ ) are scattered by the local interstellar medium (ISM). Readhead & Hewish (1972) measured the angular diameters of high-latitude extragalactic radio sources and found that their angular sizes decreased smoothly with galactic latitude. They suggested that the scattering material is uniformly distributed above the galactic plane with a scale height of  $\approx 500$  pc. In contrast, Hajivassiliou (1993) found in a similar survey that a model in which all scattering occurs at the edge of the Local Bubble could explain the measured distribution of angular diameters at high latitude. The Local Bubble is a cavity of hot coronal gas roughly 30-200 pc in extent that surrounds the earth (Cox & Reynolds 1987). Nearby pulsars tend to have stronger refractive scattering on shorter timescales (Gupta, Rickett, & Coles, 1994) and more instances of multiple imaging (Gupta, Rickett, & Lyne 1994) than more distant pulsars. This may indicate that the distribution of material responsible for scattering differs in the two cases. One possibility is that nearby pulsars are scattered by the material at the surface of the Local Bubble, while more distant pulsars are scattered by a uniform medium. In this paper we describe a measurement to determine the location of material responsible for scattering nearby pulsars.

## 2. INTERFEROMETRIC MEASUREMENTS OF ANGULAR BROADENING

The large intensity variations of pulsars in both time and frequency result from scattering by electron density fluctuations in the ISM (Scheuer 1968). Fluctuations in the interstellar electron density produce fluctuations in the index of refraction, thereby inducing variations in the relative phases of light rays propagating along different paths. The electric field measured at an antenna will vary as the phasor sum of these rays randomly coheres and decoheres. Rays that cohere at frequency  $\nu$  and time  $t$  remain coherent over a range of frequencies  $\Delta\nu$  about  $\nu$  and over a range of times  $t_{\text{iss}}$  about  $t$ . Here  $\Delta\nu$  is the scintillation bandwidth and  $t_{\text{iss}}$  is the scintillation timescale. An intensity maximum of bandwidth  $\Delta\nu$  and duration  $t_{\text{iss}}$  is called a “scintle”.

An interferometer measures the visibility, which is the complex product of the electric fields at two antennas. Because the electric field at each antenna fluctuates, the visibility  $V(\vec{x}, \vec{x} + \vec{B}; \omega, t)$  will be a function of the location of the two antennas, the frequency  $\omega$ , and the time  $t$ . Here  $\vec{x}$  and  $\vec{x} + \vec{B}$  are the positions of the antennas projected into the plane

perpendicular to the line of sight to the source. Averaging this visibility over position  $\vec{x}$  gives

$$\langle V(\vec{x}, \vec{x} + \vec{B}; \omega, t) \rangle = V_o \exp \left[ -\frac{1}{2} \langle (\phi(\vec{x}) - \phi(\vec{x} + \vec{B}))^2 \rangle \right] \quad (1)$$

where  $V_o$  is the average intensity measured at a single antenna and  $\phi(\vec{x})$  is the phase of the electric field at position  $\vec{x}$ . The equality follows from Mercier's theorem. We expect visibility fluctuations to be a stationary random process, so that averaging over  $\vec{x}$  is equivalent to averaging over many scintles in time or frequency. The angular brackets  $\langle \rangle$  indicate both kinds of averaging. We denote this averaged visibility as  $V(\vec{B})$ .

The average visibility  $V(\vec{B})$  is also the two-dimensional Fourier transform of the sky brightness distribution  $I(\vec{q})$ , where  $\vec{B}$  and  $\vec{q}$  are conjugate variables. Expressions for  $V(\vec{B})$  have been derived for several different power spectra of electron density fluctuations; we use the results of Coles et al. (1987). For a power-law spectrum of density fluctuations with index  $\alpha$  and inner scale  $l_i$

$$V(\vec{B}) = V_o \exp \left[ -\frac{1}{2} \left( \frac{\pi}{\sqrt{2 \ln 2}} \frac{\theta_H |\vec{B}|}{\lambda} \right)^{\alpha_{\text{vis}} - 2} \right] \quad (2)$$

where  $\theta_H$  characterizes the angular diameter of the average scattering disk and  $\lambda = 92$  cm is our observing wavelength. The index  $\alpha_{\text{vis}} = \alpha$  if  $|\vec{B}| > l_i$ , and  $\alpha_{\text{vis}} = 4$  if  $|\vec{B}| < l_i$ . Estimates for the inner scale range from  $10^2$  km (Spangler & Gwinn 1990, Molnar et al. 1995) to  $10^6$  km (Coles et al. 1987). We take  $\alpha_{\text{vis}} = 4$  in this paper, corresponding to a Gaussian sky brightness distribution. In this case  $\theta_H$  is the full width at half maximum (FWHM) angular diameter of the average scattering disk. Comparison of Equations 1 and 2 yields  $\theta_H$ :

$$\theta_H = \left( \frac{2 \ln 2}{\pi^2} \frac{\lambda^2}{|\vec{B}|^2} D_\phi(\vec{B}) \right)^{\frac{1}{2}} \quad (3)$$

where  $D_\phi(\vec{B}) = \langle (\phi(\vec{x}) - \phi(\vec{x} + \vec{B}))^2 \rangle$  is the phase structure function.

### 3. OBSERVABLE CONSEQUENCES OF SCATTERING

A comparison of angular broadening and temporal broadening provides information on the distribution of scattering material. Expressions for the rms scattering angle  $\theta$  and the mean broadening time  $t$  of rays propagating through a distribution of scattering material have been derived by Alcock & Hatchett (1978) and Blandford & Narayan (1985).

$$\theta^2 = \frac{1}{D^2} \int_0^D dz z^2 \psi(z) \quad (4)$$

$$t = \frac{1}{2cD} \int_0^D dz z (D - z) \psi(z) \quad (5)$$

Here  $z$  is a coordinate from the source at  $z = 0$  to the observer at  $z = D$ ,  $\psi(z)$  is the scattering rate per unit length, and  $c$  is the speed of light. The rms angular diameter of the average scattering disk is  $\theta$ , and is related to the FWHM angular diameter  $\theta_H$  by  $\theta_H = \sqrt{4 \ln 2} \theta$  if  $\alpha = 4$ . The mean broadening time  $t$  differs from the temporal broadening  $\tau$  by a factor close to unity (Lee & Jokipii 1975), which we neglect. If we assume a model of the scattering material  $\psi(z)$  with one or two parameters, we can use measurements of  $\theta_H$  and  $\tau$  to derive the values of these parameters.

In this paper we consider two special cases. If the scattering material is uniformly distributed along the line of sight,  $\psi(z)$  is a constant and the FWHM angular diameter of the average scattering disk is  $\theta_u = (16 \ln 2 c \tau / D)^{1/2}$ . If the scattering material is concentrated in a thin screen located a distance  $d_s$  from earth,  $\psi(z) \propto \delta(z - D + d_s)$  and the FWHM angular diameter of the average scattering disk is  $\theta_s = (8 \ln 2 c \tau (D - d_s) / D d_s)^{1/2}$ . We expect  $\theta_H = \theta_u$  for a pulsar scattered by a uniform medium. If the pulsar is scattered by a thin screen, we can use  $\theta_H$  and  $\tau$  to compute the distance  $d_s$  to the screen.

If the scattering material is concentrated in a thin screen, measurement of the proper motion velocity  $\vec{V}_{\text{pm}}$  of a pulsar provides an estimate of the velocity  $\vec{V}_{\text{scr}}$  of the scattering screen. Gupta et al. (1994) have discussed this relationship, which in our notation becomes

$$\frac{|d_s \vec{V}_{\text{pm}} - D \vec{V}_{\text{scr}}|}{D - d_s} = \frac{\lambda}{t_{\text{iss}}} \sqrt{\frac{D d_s \Delta \nu}{2 \pi c (D - d_s)}} \quad (6)$$

Here all velocities are measured relative to the sun and we have assumed that the earth's orbital velocity is negligible. Gupta (1995) showed that the scattering properties and proper motion velocities of most pulsars are consistent with a screen halfway to the pulsar if  $\vec{V}_{\text{scr}} = 0$ . By measuring the distance  $d_s$  to the screen, we can estimate the velocity  $\vec{V}_{\text{scr}}$  of the scattering material.

#### 4. OBSERVATIONS AND DATA REDUCTION

We attempted to resolve the scattering disks of 16 nearby pulsars with an intercontinental VLBI array. Our array consisted of telescopes at Jodrell Bank (76 m), Westerbork (phased array), Noto (30 m), and four 25 meter telescopes from the US Very Long Baseline Array of the National Radio Astronomy Observatory<sup>1</sup>: Hancock, Owens

---

<sup>1</sup>NRAO is operated by the Associated Universities Inc., under contract with the National Science Foundation.

Valley, Brewster, and St. Croix. We observed for 12 hours on 1994 May 25-26, recording left-circular polarization from 323 to 337 MHz with the Mark IIIA VLBI recording system. The observations were broken into 13 minute scans, and alternated between the pulsars and a set of extragalactic radio sources used for calibration. We detected only 2 calibration sources, 1345+125 and 2230+114, on intercontinental baselines.

The tapes were correlated with the Mark IIIA correlator at the Max-Planck Institut für Radioastronomie in Bonn, Germany. We integrated the data over 2.5 second intervals and correlated over 24 lags, yielding 0.167 MHz frequency resolution. This is sufficient to resolve typical scintillation bandwidths of nearby pulsars at 326 MHz (see Table 1). Pulsar gating allowed us to correlate only during the pulse, yielding an improvement in the signal to noise ratio by a factor of 2-5 (Gwinn et al. 1986). The data from Hancock were discarded due to poor recording quality.

We used Haystack Observatory’s fringe fitting program FOURFIT to recover the cross-correlation functions from the Mark IIIA correlator output files. These were Fourier transformed to give the visibility  $V(\vec{x}, \vec{x} + \vec{B}; \omega, t)$ .

The visibility data were degraded by the fractional bitshift effect. This effect arises from the inability of a lag correlator to adjust the digitized data streams continuously to compensate for the variation of the geometrical delay  $\tau_g(t)$ . The sawtooth error in delay  $\Delta\tau_g(t)$  causes a phase error  $\phi_{\text{fbs}}(\omega, t) = \omega\Delta\tau_g(t)$ . This error nearly averages out for unmodulated sources, but we found that beating between  $\phi_{\text{fbs}}(\omega, t)$  and the pulse gate introduced errors in the phases of as much as 0.5 radians. We computed the corrections to the visibility phases by reconstructing the sawtooth delay error from the Mark IIIA correlator output and matching it to the pulsar ephemeris.

For each baseline in each scan we removed an instrumental model from the visibility phase. This model corrected for the phase errors introduced by the differing electronic pathlengths of the seven 2 MHz baseband converters, the geometrical delay, and the passband curvature within the baseband converters. Our phase correction for the geometrical delay contained 3 contributions: the multiband delay, the fringe rate, and the multiband acceleration. This last correction is not normally removed in interferometry, but was found to introduce errors of up to 0.5 radians on some baselines. The phase passband curvature of the baseband converters,  $\phi_{\text{pb}}(\omega)$ , was computed for each baseline by time averaging the visibility phases over the entire data set. These corrections were  $\leq 0.2$  radians. The resulting visibility phases were stable to 0.1 radians for our brightest sources.

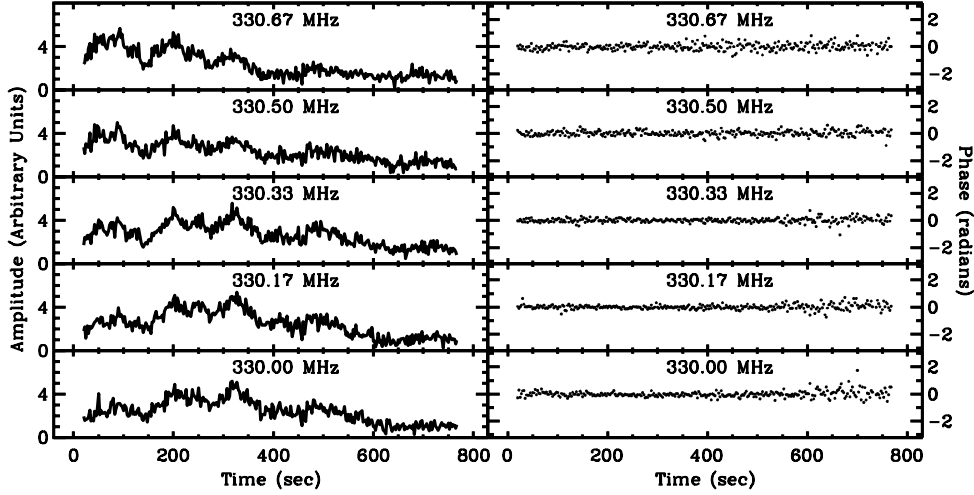


Fig. 1.— The visibility of the pulsar B1919+21 plotted for the 7812 km Owens Valley - Westerbork baseline. On the left the visibility amplitude is plotted vs. time for 5 adjacent frequency channels out of 85 observed. The amplitude shows variations in both time and frequency caused by scattering in the ISM. The visibility phase is plotted vs. time on the right, and shows no such variations. This indicates that the scattering disk of the pulsar is unresolved on this baseline. The small fluctuations in the phase are consistent with noise.

## 5. RESULTS

Although we detected fringes on all but one of the 16 pulsars we observed, only the 5 listed in Table 1 were bright enough to resolve individual scintles. All pulsars and quasars showed strong fluctuations of visibility phase with a bandwidth greater than 14 MHz. Scattering by the ionosphere and the interplanetary medium caused these fluctuations. Ananthakrishnan & Dennison (1989) saw this effect in an observation of 3C 286. These phase fluctuations contain information on the strength and spectral index of electron density fluctuations in the solar wind (Cronyn 1972), and will be analyzed in a subsequent paper. We removed this effect by subtracting a phase  $\phi_{bb}(t)$  averaged in frequency over the 14 MHz bandwidth of our experiment. Since  $\Delta\nu \leq 1$  MHz for our sources we expect this not to affect the visibility phase fluctuations associated with interstellar scattering.

The visibility of the pulsar 1919+21 on the 7812 km Owens Valley - Westerbork baseline is plotted in Figure 1. The visibility amplitude shows fluctuations in both time and frequency characteristic of scattering by the ISM. The visibility phase shows no such variations, indicating that the scattering disk of the pulsar is unresolved on this baseline. We computed the autocorrelation function of the real and imaginary components of the visibility, and used the single-point offset to measure the phase structure function (Gwinn

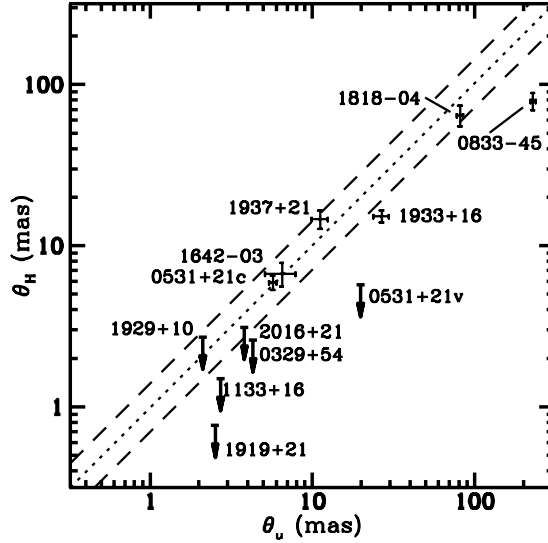


Fig. 2.— The observed FWHM angular diameter  $\theta_H$  of the average scattering disk plotted vs. the FWHM angular diameter  $\theta_u$  expected for scattering through a uniform medium. If a uniform medium is responsible for the scattering of these pulsars, points will lie on the dotted line  $\theta_H = \theta_u$ . The dashed lines delimit the range of error in  $\theta_u$  caused by a factor of 2 uncertainty in pulsar distances. The angular diameters of three nearby pulsars are inconsistent with a uniform distribution of scattering material.

et al. (1996)).

$$D_\phi = \frac{\langle (\text{Im}[V(\vec{x}, \vec{x} + \vec{B}; \omega, t)])^2 \rangle}{4 \langle (\text{Re}[V(\vec{x}, \vec{x} + \vec{B}; \omega, t)])^2 \rangle} \quad (7)$$

The single-point offset of the phase autocorrelation function suppresses noise, but preserves the contribution from interstellar scattering because these fluctuations correlate over many points in time and frequency. We were unable to detect visibility phase fluctuations for any of the 5 pulsars. Table 1 lists upper limits on  $D_\phi$  and  $\theta_H$  and lower limits on  $d_s$ .

In Figure 2 we plot  $\theta_H$  vs.  $\theta_u$  for 11 pulsars. All detections are taken from Gwinn et al. (1993) and references therein. The upper limits are from Table 1 except for the pulsar 0531+21v. This upper limit represents the angular broadening  $\theta_u$  associated with the long term variable component of the Crab pulsar’s temporal broadening  $\tau$ . Isaacman & Rankin (1977) found both a variable component and a steady component in the temporal broadening of this pulsar. The variable component of  $\tau$  changes on timescales of months to years, and is thought to be due to scattering within the Crab supernova remnant. The steady component of  $\tau$  arises from scattering in the ISM, and the associated angular broadening  $\theta_u$  is signified by 0531+21c. The measured angular broadening of this pulsar is consistent with scattering in the ISM (Vandenberg 1976).

## 6. DISCUSSION

The scattering properties of most distant pulsars are consistent with scattering through a uniform medium. The two exceptions are the young pulsars 0531+21v and 0833-45. These pulsars are scattered by their enclosing supernova remnants, and the large distance to these remnants produces scattering disks with smaller angular diameters. The scattering disks of the three nearby pulsars 0329+54, 1133+16, and 1919+21 are too small to be due to scattering in a uniform medium. If the scattering material is concentrated in a thin screen, the lower limits on  $d_s$  for the pulsars 0329+54, 1919+21, and 2016+28 preclude scattering from the surface of the Local Bubble. With the exception of 1133+16, all pulsars in Table 1 have galactic latitudes  $|b| < 5^\circ$ . Like low-latitude extragalactic radio sources these pulsars might be scattered by HII regions or supernova remnants in the galactic disk. However, it seems unlikely that all of them would be scattered by small features close to the pulsars. We can use the lower limit on  $d_s$  to compute a lower limit on the component of the velocity  $\vec{V}_{\text{scr}}$  of such a feature. This lower limit occurs when the screen is moving in the same direction as the pulsar. These lower limits appear in Table 1, and indicate that the scattering material must be moving in the same direction as the pulsar. While the required velocities for the scattering material are not large, they suggest that the scattering material may be associated with the pulsar.

To explain these results, we argue that material close to the pulsar dominates the scattering for nearby pulsars, producing small scattering disks. This scattering could be caused by strong electron density fluctuations present at the shock front between an electron positron wind and the ambient ISM. Relativistic winds from pulsars can produce X-ray synchrotron nebulae (Cheng & Helfand 1983, Seward & Wang 1988), indicating the possible presence of such a shock front. The pulsar 2224+64 is an example of an older high velocity pulsar that has long since left its supernova remnant and whose wind has evacuated a cavity in the ISM (Cordes 1993). These relativistic winds may be present at low levels in all pulsars, but may nevertheless induce the dominant electron density fluctuations for these nearby pulsars.

For more distant pulsars the integrated interstellar electron density fluctuations grow to dominate the scattering, and produce scattering disks consistent with a uniform distribution of scattering material. In this model the Crab pulsar would be an intermediate case, in which the ISM dominates the angular broadening but the effects of scattering in the supernova remnant are apparent in the variable component of the temporal broadening.

We thank Omer Blaes and Jon Arons for several useful discussions. This work was supported in part by the National Science Foundation grant AST 92-17784.



Table 1. Scattering Properties of Nearby Pulsars

Pulsar (B1950)	$D^a$ (pc)	$\Delta\nu^b$ (MHz)	$\tau^c$ ( $\mu$ s)	$\theta_u$ (mas)	$ \vec{B} $ (km)	$D_\phi^{1/2}$ (rad)	$\theta_H$ (mas)	$d_s$ (pc)	$t_{\text{iss}}^d$ (s)	$ \vec{V}_{\text{pm}} ^d$ (km/s)	$ \vec{V}_{\text{scr}} $ (km/s)
0329+54	1430	0.028	5.7	4.3	5730	<0.21	<2.6	>820	146	145	>4
1133+16	270	0.43	0.37	2.7	7870	<0.17	<1.5	>160	77	475	>50
1919+21	660	0.17	0.92	2.5	7810	<0.085	<0.77	>560	150	122	>9
1929+10	170	0.99	0.16	2.1	7940	<0.30	<2.7	>39	351	86	...
2016+28	1100	0.046	3.5	3.8	6510	<0.28	<3.1	>470	463	12	...

<sup>a</sup> Distances are from Taylor, Manchester & Lyne (1993).

<sup>b</sup> Scintillation bandwidths are from Cordes (1986) and have been scaled to 326 MHz using the relation  $\Delta\nu \propto \nu^{4.4}$ .

<sup>c</sup> Broadening times are calculated using the relation  $\tau = 1/2\pi\Delta\nu$ .

<sup>d</sup> Scintillation timescales and proper motion velocities are taken from Gupta (1995). Scintillation timescales have been scaled to 326 MHz using the relation  $t_{\text{iss}} \propto \nu^{1.2}$ .

## REFERENCES

- Alcock, C. & Hatchett, S. 1978, 222, 456
- Ananthakrishnan, S., & Dennison, B. 1989, in *Radio Astronomical Seeing*, ed. J.E. Baldwin and Wang S.-G., Beijing: International Academic, 205
- Blandford, R. & Narayan, R. 1985, MNRAS, 213, 591
- Cheng, A. F. & Helfand, D. J. 1983, ApJ, 271, 271
- Cox, D. P. & Reynolds, R. J. 1987, ARA&A, 25, 303
- Coles, W. A., Frehlich, R. G., Rickett, B. J., & Codona, J. L. 1988, ApJ, 315, 666
- Cordes, J. M. 1986, ApJ, 311, 183
- Cordes, J. M., Romani, R. W., & Lundgren, S. C. 1993 Nature, 362, 133
- Cordes, J. M., Weisberg, J. M., & Boriakoff, V. 1985, ApJ, 288, 221
- Cronyn, W. M. 1972, ApJ, 174, 181
- Dennison, B., Thomas, M., Booth, R. S., Brown, R. L., Broderick, J. J., & Condon, J. J. 1984, A&A, 135, 199
- Desai, K. M., Gwinn, C. R., Reynolds, J., King, E. A., Jauncey, D., Flanagan, C., Nicolson, G., Preston, R. A. & Jones, D. L. 1992, ApJ, 393, L75
- Gupta, Y. 1995, ApJ, 451, 717
- Gupta, Y., Rickett, B. J. & Coles, W. A. 1993, ApJ, 403, 183
- Gupta, Y., Rickett, B. J. & Lyne, A. G. 1994, MNRAS, 269, 1035
- Gwinn, C. R., Bartel, N. & Cordes, J. M. 1993, ApJ, 410, 673
- Gwinn, C. R., Ojeda, M. J., Britton, M. C., Reynolds, J. E., Jauncey, D. L., King, E. A., McCulloch, P., Lovell, J. E. J., Flanagan, C. S., Smits, D. P., Preston, R. A., & Jones, D. L. 1996, ApJ, submitted
- Gwinn, C. R., Taylor, J. H., Weisberg, J. M., & Rawley, L. A. 1986, AJ, 91, 338
- Hajivassiliou, C. A. 1992, Nature, 355, 232
- Isaacman, R. & Rankin, J. M. 1977, ApJ, 214, 214
- Lee, L. C. & Jokipii, J. R. 1975, ApJ, 201, 532
- Molnar, L. A., Mutel, R. L., Reid, M. J. & Johnston, K. J. 1995, ApJ, 438, 708
- Moran, J. M., Rodríguez, L. F., Greene, B. & Backer, D. C. 1990, ApJ, 348, 147
- Rao, A. P. & Ananthakrishnan, S. 1984, /nat, 312, 707

- Readhead, A. C. S. & Hewish, A. 1972, *Nature*, 236, 440
- Scheuer, P. A. G. 1968, *Nature*, 218, 920
- Seward, F. D. & Wang, Z. R. 1988, *ApJ*, 199, 332
- Spangler, S. R. & Gwinn, C. R. 1990, *ApJ*, 353, L29
- Spangler, S. R., Mutel, R. L., Benson, J. M. & Cordes, J. M. 1986, *ApJ*, 301, 312
- Taylor, J. H., Manchester, R. N., & Lyne, A. G. 1993, *ApJS*, 88, 529
- Vandenberg, N. R., Clark, T. A., Ericson, W. C. & Resch, G. M. 1976, *ApJ*, 207, 937